Synthesis, characterization, and magnetic properties of defective nitrogen-doped multiwall carbon nanotubes encapsulating ferromagnetic nanoparticles

María Luisa García-Betancourt[1, a], Yadira Vega-Cantu[1,2,b], Sofía M. Vega-Díaz[3,c], Aaron Morelos-Gómez[5,d], Nestor Perea-López[4,e], Rodolfo Cruz-Silva[3,f], Humberto Gutiérrez[4,g], Humberto Terrones[3,h], Mauricio Terrones[3,4,6i] and Emilio Muñoz-Sandoval[1,j]

[1]Advanced Materials Division, IPICYT, Camino a la Presa San Jose 2055, SLP, SLP, 78216, Mexico

[2]Department of Chemistry, Federal University of Pernambuco, Cidade Universitária, Recife, PE, 50670-901, Brazil

[3]Research Center for Exotic Nano Carbons (JST), Shinshu University, 4-17-1 Wakasato, Nagano City 380-8553, Japan.

[4] Department of Physics and Center for 2-Dimensional and Layered Materials, The Pennsylvania State University, University Park, PA 16802-6300, USA

[5]Institute for carbon Science and Technology, Shinshu University, 4-17-1 Wakasato, Nagano City 380-8553, Japan

[6]Department of Chemistry, Department of Materials Science and Engineering & Materials Research Institute, The Pennsylvania State University, University Park, PA 16802-6300, USA

[a]luisa.garcia@ipicyt.edu.mx, [b]yivega@ipicyt.edu.mx, [c]smvd@shinshu-u.ac.jp, [d]amorelosg@gmail.com, [e]nup13@psu.edu, [f]rcruzsilva.rcen@gmail.com, [g]hur3@psu.edu, [h]hzt2@psu.edu, [i]mut11@psu.edu, [j]ems@ipicyt.edu.mx (corresponding author)

[Don't type anything in this line, it'll show the date of receipt and acceptance]

Keywords: carbon nanotubes; defects; chemical vapor deposition; metallic nanoparticles; magnetic properties.

Abstract. Nitrogen-doped multi-walled carbon nanotubes (CN_xMWNTs) with multiple morphological defects were produced by a chemical vapor deposition (CVD) method. An aqueous solution of NaCl (26.82 wt%) was used instead of acetone in the trap that is typically used to catch organic byproducts from carbon pyrolysis in the synthesis of carbon nanotubes. Carbon nanotubes with sharp tips and lumps were produced following this modification in the synthesis process. Scanning electron microscopy (SEM) and high-resolution transmission electron microscopy (HR-TEM) showed the presence of nanoparticles of several shapes inside the nanotubes. The electronic and magnetic properties were studied using a Physical Properties Measurement Evercool system (PPMS). With this simple change in the CVD-trap it was possible to modify the morphology of carbon nanotubes and of encapsulated metallic nanoparticles. The differences in gas flow are proposed as the possible mechanism to produce these changes in both the nanoparticles and CN_xMWNTs.

Introduction

It is well known that defects affect the crystalline structure of graphitic lattice of carbon nanotubes; however, different studies have shown the advantage of specific defects on the CNT morphology in their electronic and other physical properties [1-3]. For example, native defects produced during the synthesis, such as dangling bonds, vacancies or sp^3 hybridizations; promote the anchorage of molecules on the CNTs walls [4]. On the other hand, structural defects on CNTs due to branching or bundle formation lead to junctions, which could be useful in the field of electronics [5,6] and composites reinforcement [7]. Other types of "defects" such a heteroatoms (extrinsic defects), can be incorporated into CNTs by intercalation, encapsulation or substitution [8]. This modifies their electronic and physico-chemical properties. One of the challenges in this context is to control the synthesis of "defective" CNTs.

Depending on their origin, defects can be classified into induced or produced. Induced defects can be tailored by damaging non-defective CNTs, producing new carbon nanostructures. Some methods used for this end are: i) electron or ion irradiation which produce reactive sites on CNTs walls [9,10]; and "solder" CNTs forming junctions [11] or nanolumps [12]. ii) Ion intercalation, such as lithium in ammonia, exfoliate MWCNTs resulting in carbon nanoribbons [13]. And iii) nanoparticle deposition on the external CNTs walls, can lead to formation of lumpy nanostructures [14,15].

On the other hand, produced defects are mainly originated during the synthesis. CVD is a method which can be easily modified to produce defective CNTs by altering several specific parameters in the experimental setup, such as solution precursors, temperature, gas flow, deposition time. For instance, changing doping level by changing growth conditions of CNT modulates the dimensions of the "bamboo" compartments in nitrogen doped CNTs [16-17] and coalesced CNTs can be produced by changing the solution precursor during microwave-assisted CVD [18]. Junctions can be produced by changing the flow of the carrier gas [19] or simply by changing growth temperatures to induce coalescence of metallic nanoparticles [20]. High temperature, combined with a high catalyst concentration promotes the agglomeration of carbonaceous and metallic nanoparticles on CNTs surfaces [21]. In this regard the shape of nanoparticles attached to the walls (nanolumps) [22] or encapsulated in the CNTs [23,24] modifies the structure and properties of CNTs

In this paper, following our previous work [25], we present the formation of nitrogen-doped multiwalled carbon nanotubes with different morphologies, resulting from a slightly modification of the typical CVD synthesis method. Instead of using acetone in the bubbler (uses as a trap for volatiles at the exit of the quartz tube reactor), an aqueous solution of NaCl (26 wt% of NaCl) was employed. We believe that the formation of these new defects is due to changes in the gas flow, since it is a crucial parameter in transporting the catalyst and the carbon precursor into the reactor.

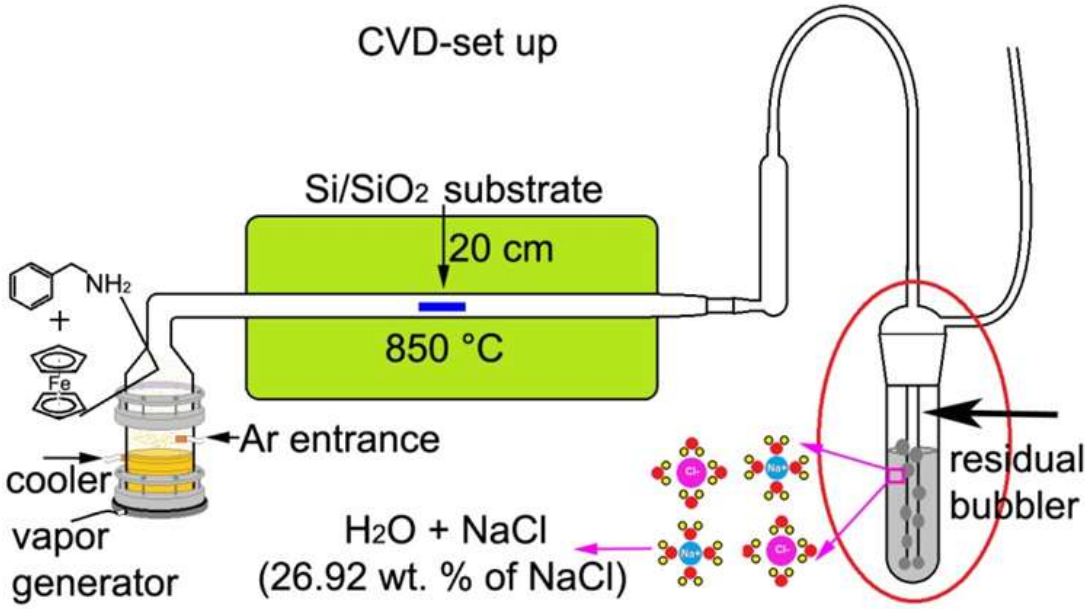

Fig. 1. Schematic picture of the modified chemical vapor deposition method (CVD) used for the synthesis of defective CN_xMWNTs. The red oval encloses the residue bubbler (trap) where aqueous solution of NaCl was used instead of acetone.

Experimental

Nitrogen-doped multiwall carbon nanotubes (CN_xMWNTs) were produced by spray pyrolysis using a chemical vapor deposition (CVD) set-up consisting of one tubular furnace (configuration shown in Fig. 1). The organometallic ferrocene ($FeCp_2$- Sigma Aldrich, precursor for catalytic Fe nanoparticles), was dissolved at 6 wt % in the organic solvent benzylamine (C_7H_9N- Sigma Aldrich, source of C and N). This solution was nebulized by an ultrasound pulse-generator and transported by an argon flow of 2.5 L/min inside the quartz tube and pyrolized at 850 °C during 30 min. CN_xMWNTs were collected from a piece of silicon substrate (with a native oxide surface) placed inside the quartz tube at the middle of the furnace (20 cm from entrance); where the temperature is more stable. A solution of water and NaCl (26.92 wt. %) was placed in the bubbler (red oval enclosed in Fig. 1) used to catch volatile organic residues. CN_xMWNTs collected from the quartz tube were placed directly in X ray difractometer (Bruker D8 Advance) for XRD studies. Afterwards, the substrate was cut in half to observe a cross-sectional view of the CN_xMWNTs forest in a Scanning Electron Microscope, (SEM, FEI XL 30 SFEG). Then, CN_xMWNTs were scrapped from the silicon substrate and

characterized by High-Resolution Transmission Electron Microscopy (HRTEM, FEI TECNAI F30). Thermogravimetric analysis (TGA) and Raman spectroscopy (using a 514 nm laser line) were performed as well. Finally, a piece of substrate (1.0 cm by 0.5 cm) containing a forest of CN_xMWNTs was placed in a PPMS (Quantum Design EverCool) in order to study their magnetic properties. For four-wire resistance measurements, a smaller piece of substrate (3.3 X 7.7 mm) was mounted on the standard PPMS sample puck. Four thin Cu wires (100 μm) were placed on in contact with the upper surface of the CNT forest and connected to the four contacts of the PPMS-puck.

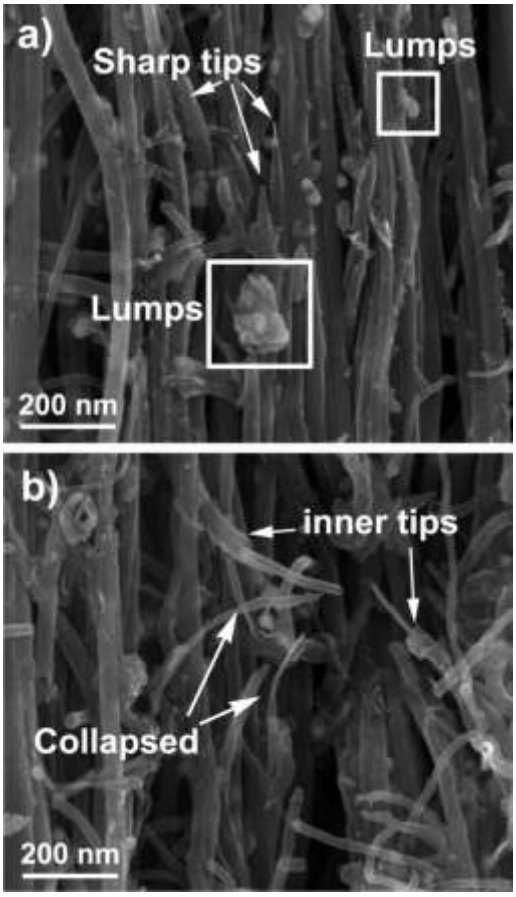

Fig. 2. SEM images of defective CN_xMWNTs synthesized with 26.9 wt% aqueous solution of NaCl in the bubbler. The images show the typical morphologies: (a) sharp tips (arrows) and "lumps" (squares); (b) collapsed thin CN_xMWNT emerging from broken nanotubes forming inner tips (arrows).

Results

Fig. 2 displays an overview of SEM images of samples of CN_xMWNTs forests synthesized as described above. In Fig. 2a the arrows point up broken CN_xMWNTs with sharp tips and the squares enclose external nanoparticles deposited over the CN_xMWNT surface ("lumps"). Fig. 2b shows thin CN_xMWNTs emerging from thicker nanotubes, which apparently were broken (labeled "inner tips" in Fig. 2a). Additionally, in Fig. 2b some of these sharp tips appear to be collapsed. The morphology of this sample is dramatically different from a control sample of CN_xMWNTs synthesized using acetone in the residual bubbler where the carbon nanotubes have smooth surfaces (Fig. 3a) and regular tubular shapes (Fig. 3b). The diameter distribution of the sample produced by our typical CVD method (acetone filled trap), is different with a larger average diameter than for CN_xMWNTs synthesized with NaCl solution in the trap. Fig. 3c shows that for "conventional" CN_xMWNT conical nanoparticles appear at the tip of the nanotube and the rest of these CN_xMWNTs is typically empty (Fig. 3d), with the inner walls typically "bamboo-shaped", with wall compartments that can be very thin (Figs. 3d and 3e), or well-defined with several graphitic layers (Fig. 3f).

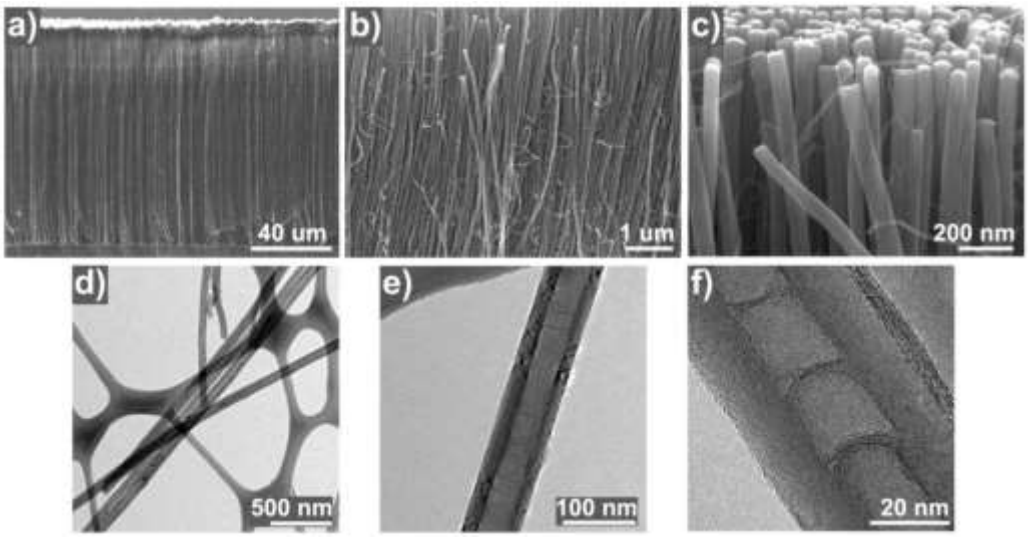

Fig. 3. Scanning electron microscopy images of nitrogen doped carbon nanotubes CN_xMWNTs synthesized by CVD using an acetone filled trap: **(a)** perpendicular and highly aligned growth onto the Si/SiO_2 substrate; **(b)** general view of the carbon nanotubes morphology; **(c)** high magnification SEM image of CN_xMWNTs containing catalytic particles at their ends, the CN_xMWNTs diameter is ~ 70 nm; **(d)** HRTEM of CN_xMWNTs; **(e)** HRTEM image showing the morphology of individual CN_xMWNTs where the bamboo compartments are barely visible; **(f)** HRTEM image showing the typical bamboo morphology of CN_xMWNTs.

Table 1. Summary of morphologies, shapes, dimensions and relative abundance of metallic catalyst nanoparticles encapsulated in carbon nanotubes synthesized using aqueous solution of NaCl at 26.92 wt.% . 50 HRTEM images and 100 nanoparticles encapsulated in CNT were measured.

Nanoparticle shape	**Diameter interval (nm)**	**Length interval (nm)**	**Percentage (%)**
spherical	5-22	-	13
cylindrical	7-20	7-52	28
deformed	4-23	81-118	23
seed	8-20	23-97	28
oval	4-12	18-39	5
arrow	4-14	20-68	3

Fig. 4 shows several HRTEM images of defective CN_xMWNTs, produced using an aqueous solution of NaCl to fill the trap, showing encapsulated metal nanoparticles which take different shapes: spherical (Fig 4a), cylindrical (Fig. 4b), “deformed” (Fig. 4c), seed-type (Fig. 4d), oval (Fig 4e) and arrow-type (Fig. 4f). Table 1 summarizes size and frequency of the different particle morphologies. Fig. 4a shows the end of a broken CN_xMWNT containing a spherical-shaped nanoparticle on the tip (22 nm diameter). This particular type of nanoparticle represents *ca.* 13% in the sample (see Table 1). Fig. 4b presents an encapsulated metallic nanoparticle with a cylindrical shape of approximately 40 nm in length and 11 nm in diameter. Cylindrical shapes account for approximately 28% of the formed nanoparticles (see Table 1). Another nanoparticle shape relatively abundant is the "deformed" morphology. These nanoparticles can be considered as the union of two nanoparticles (see Fig. 4c) or they might result from cylindrical nanoparticles that experienced a necking process (see inset Fig. 4c). Seed-type nanoparticles can be also formed inside the CN_xMWNTs, these are usually wider than the CN_xMWNT internal diameter (see Fig. 4d). Apparently, these nanostructures can be formed by coalescence of several nanoparticles, but evidence of this process is still inconclusive. Nanoparticles are not only found in the core of the nanotubes, but also oval-type nanoparticles were found on the walls, although in smaller amounts (see Fig. 4e). As

can be observed, the particle appears between the walls of the graphitic layers, and voids can be observed next to the nanoparticle along the axis of the nanotube. These oval-type nanoparticles were most likely formed by the coalescence of small nanoparticles initially anchored to the CN_xMWNT walls during the synthesis. Finally, Fig.4f presents an encapsulated metallic nanoparticle with an "arrow" morphology having a thickness of approximately 8 nm, a length of ~ 59 nm and the diameter at its base of ~20 nm. Such nanoparticles represent only 3% of the total observed shapes and might result from capillary filling of a small inner diameter nanotube section.

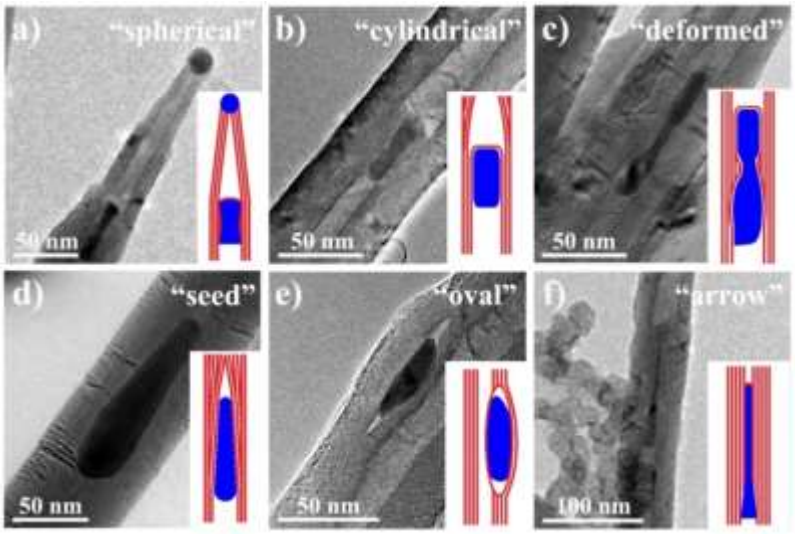

Fig. 4. High-resolution transmission electron microscopy images of encapsulated metallic nanoparticles present in CN_xMWNTs synthesized using a NaCl solution filled trap. The inset in each image is a drawing that represents the shape of each corresponding nanoparticles. The shape of nanoparticles can be: (a) "spherical" nanoparticle at the tip of sharp broken CN_xMWNTs attached at the end of the long compartment (b) "cylindrical" nanoparticles encapsulated in CN_xMWNTs (c) "deformed" nanoparticles which are encapsulated also are relatively (d) "seed" like nanoparticle encapsulated within CN_xMWNTs (e) "oval" nanoparticles encased on the CN_xMWNTs walls, most likely due to the formation of twin carbon nanotubes; (f) Rare "arrow" encapsulated nanoparticles displaying a sharp tip that fills a narrow core section of a nanotube.

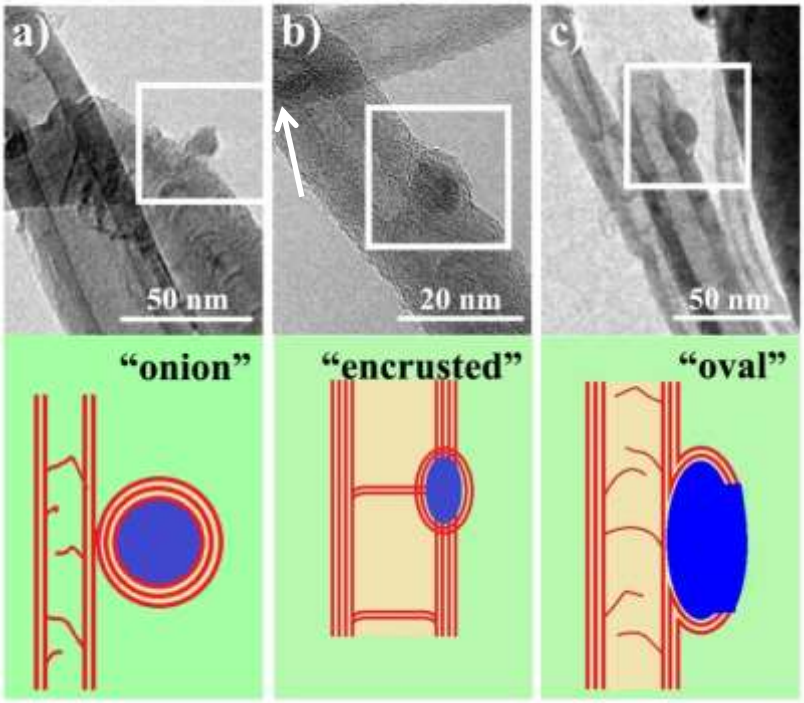

Fig. 5. HRTEM images of lumps attached in CN_xMWNT surfaces with different morphologies represented with drawings. (a) Onion-like lump with multi-shell carbon nanostructure encapsulating a metallic nanoparticle. (b) Encrusted lump with oval shape that grew between the CN_xMWNT walls near the limit of compartments. (c) Oval-shaped lump partially uncoated attached to the CN_xMWNT outer surface.

In the literature, oval-type nanoparticles on CNTs walls are known as "nanolumps". They might result from catalytic metallic nanoclusters attached to the CN_xMWNTs surface during the nanotube growth. However; nanolumps are not truly part of a carbon nanotube; and can be considered a nanomaterial deposited on the surface. Apparently, during the synthesis of CN_xMWNT, nanolumps can seed the growth of thin carbon nanotubes if an oval particle is not formed. Such thin carbon nanotubes can be seen in Fig. 2 or Fig 3c. Typical dimensions of nanolumps range from 7 to 80 nm. Fig. 5a shows a representative "onion" nanolump with a spherical nanoparticle encapsulated by graphitic carbon layers. This onion lump has a diameter of ~11 nm; while the encapsulated nanoparticle has a diameter of ~9 nm. Fig. 4b presents an "encrusted" type nanolump. This kind of nanolump is similar to the oval-shaped nanoparticles, however; in this case, the nanoparticle is closer to the inner core of CN_xMWNT, separated only by a few (3 or 4) graphitic layers. The mechanism of formation of this particular morphology is not clearly understood, but it can result from a thin CN_xMWNT whose growth was interrupted by the formation of an additional nanoparticle, *i.e.* the

nanolump. Indeed, the nanoparticle shown on top of the image and pointed up by a white arrow could be the catalytic nanoparticle from where the CN_xMWNT was grown. In a different case, the oval nanolump (Fig. 5c) has dimensions of 9x16 nm, and is very similar to the oval-shaped nanoparticle shown in Fig. 4e, nevertheless, a very important difference is that in the oval-shaped lump, the nanoparticle is not completely coated by carbon layers, exposing the catalyst surface. This is a very important difference, since this particle can generate metallic oxides upon exposure to air, affecting the magnetic properties.

The magnetization measurements of conventional and defective CN_xMWNTs samples are shown in Fig. 6. Comparing the Figs 6a (acetone) and 6b (NaCl solution), a similar process of demagnetization can be observed in both samples. However, coercive field at 2K in the sample prepared using a trap filled with acetone (more than 0.2T) is slightly larger than the sample prepared using a NaCl solution in the trap (less than 0.2T). This difference could be associated to the heterogeneous morphologies of ferromagnetic nanoparticles when NaCl solution is used (see Fig. 4), particularly, spherical and oval shaped particles could reduce the coercive field. There is a noticeable difference the saturation of conventional CVD (acetone in the trap) and defective (NaCl solution in the bubble) CN_xMWNTs samples, (Fig. 6c) which could be associated to the combination of two factors: i) the chemical composition of encapsulated ferromagnetic nanoparticles; in samples prepared using an acetone-filled trap, the nanoparticles consist on pure iron or iron-carbide [26] in samples prepared with a NaCl solution-filled trap, the ferromagnetic nanoparticles may be contaminated reducing the content of pure iron. ii) The morphology of ferromagnetic nanoparticles is different; since the process of magnetization and demagnetization are strongly dependent on the shape and size of nanoparticles and the applied magnetic field direction [24,27].

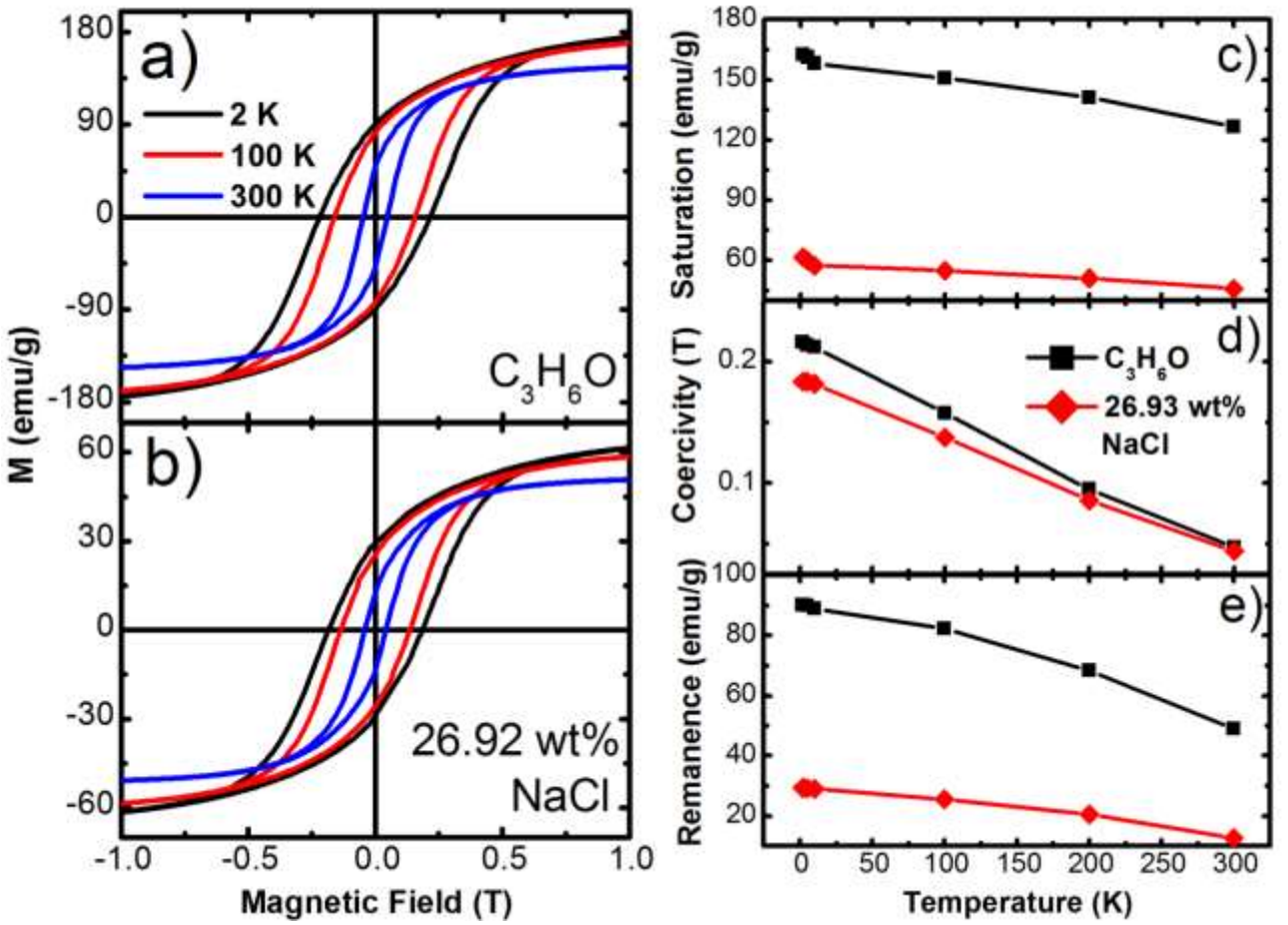

Fig. 6**.** Hysteresis loops at different temperatures (2 K, 100 K, and 300 K) for metallic nanoparticles from the CN_xMWNTs synthesized with: a) acetone filled (C_3H_6O) and b) Sodium chloride solution (26.92 wt% of NaCl in water). Evaluation of magnetic properties: c) saturation, d) coercivity and e) remanence.

During all measurements the magnetic field was applied perpendicularly to the carbon nanotubes. When doing so, the irregular shapes of smaller nanoparticles for the NaCl case could reduce the saturation magnetization due the surface or finite size effects [28,29]. A similar behavior is observed in the remanence (Fig. 6e). Additional experimental evidence is needed to understand the difference in saturation and remanence magnetic properties of samples synthetized using acetone and NaCl in the tramp. Additionally; in both cases saturation magnetization, coercivity and remanence decrease almost linearly when increasing the temperature. This behavior has been associated with the presence of anisotropy [29] or magnetoelastic effects combined with thermal fluctuations [30]. However, based on Mossbauer studies, it has been proposed that decreasing of coercive fields can be associated to a complicated distribution of phases in the samples [31]. Other Mossbauer studies show that α-Fe is

the predominant phase in double–walled carbon nanotubes [32], but Reuther et al. studies show that the sample preparation method can produce the formation of several phases such as α-Fe or iron-carbide and iron oxides [33]. In our case, a slightly different temperature dependence of coercivity is observed. This difference could be attributed to the formation of superparamagnetic nanoparticles or oxide phases in the samples fabricated with NaCl solution in the residual bubbler. As it can be seen in Fig. 6c and 6e; the decreasing of saturation magnetization or remanence is smaller as the temperature increase for samples synthetized using a NaCl solution in the trap. These small differences could be due to finite size effects[34]. A specific in depth study is necessary to clarify these behaviors.

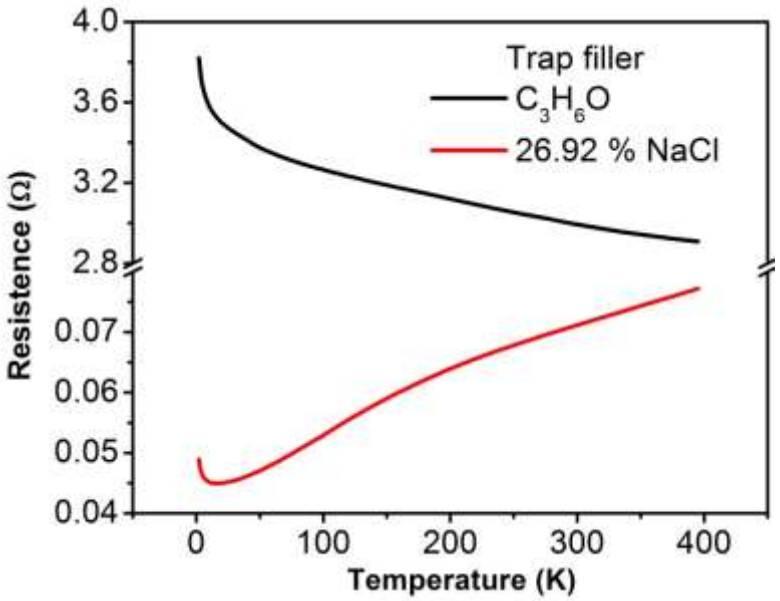

Fig. 7. Resistance behavior of CN_xMWNTs synthesized with two different CVD set-ups: trap filled with aceton (black line) and filled with NaCl solution (red line).. For the first case, resistance shows a typical semiconducting behavior. On the other hand, the sample prepared with a NaCl solution filled trap shows a metallic response above 20 K and semiconducting behavior at very low temperatures.

Finally, Fig. 7 shows the resistance behavior for both types of nanotubes. When acetone was used in the trap, the resulting CN_xMWNTs showed semiconducting electronic transport with high resistance at low temperatures (2K). However, CN_xMWNTs fabricated with NaCl solution in the trap, showed two behaviors of electronic transport: i) at very low temperatures (below 20 K) the resistance

increases when temperature decreases; ii) between 20 K and 300 K, their behavior is metallic-type. We proposed that contamination of the substrate where carbon nanotubes were grown is responsible for the morphologic transformation of carbon nanotubes and encapsulated nanoparticles. If that were the case, NaCl trace quantities traveling to the synthesis zone could have affected the produced CN_xMWNTs. This could explain the metallic transport at temperatures above 20K.

Conclusions.

We have synthesized CN_xMWNTs with multiple defects by a simple modification of the CVD method, consisting in a change of the liquid used in the residue trap. We observed changes in the CN_xMWNTs morphology that can be attributed to the encapsulated metallic nanoparticles. Those nanoparticles could affect how nanotube growth starts and the way they continue to grow during synthesis. Using an NaCl solution filled trap, electron microscopy analysis of the products showed very different shapes of nanoparticles which correlate to different CN_xMWNTs morphologies. The mass transport mechanism is still not completely understood but most likely is due to changes in the gas flow and pressure produced by the change of density of the liquid used to fill the residual tramp. We observed no significant differences in the magnetization behavior; but coercive fields, remanence and saturation of CN_xMWNTs were smaller for samples produced using a residue trap filled with a NaCl solution.

Acknowledgements.

The authors thank G. J. Labrada-Delgado, D. Ramirez-Gonzalez, F. Tristan and A.L. Elías for technical support and Dr. Fernando J. Rodríguez-Macías for help in revising the manuscript and helpful discussion. S.V.D., R.C.S. and M.T. thank JST Japan for funding the Research Center for Exotic NanoCarbons, under the Japanese Regional Innovation Strategy Program by the Excellence. M.T. thanks the support from the U.S. Air force Office of Scientific Research MURI grant FA9550-12-1-0035. E.M.S., Y.I.V.C. thank CONACYT for grant CB-2008-SEP-106942, and the Laboratory for Nanoscience and Nanotechnology Research-LINAN of IPICYT for characterization facilities;

MLGB thanks Physics Department of Penn State University and LINAN-IPICYT for facility access and CONACYT for scholarship 223824.

References

[1] Z. Yao, HWC Postma, L. Balents, C. Dekker, Carbon nanotube intramolecular junctions, Nature 402 (1999) 273-276.

[2] M.R. Falvo, G.J. Clary, R.M. Taylor, V. Chi, F.P. Washburn, R. Superfine, Bending and buckling of carbon nanotubes under large strain, Nature 389 (1997) 582-584.

[3] J.C. Charlier, Defects in carbon nanotubes, Accounts Chem. Res. 35 (2002) 1063-1069.

[4] I.Y. Jeon, D.W. Chang, N.A. Kumar, J.B. Baek, Functionalization of Carbon Nanotubes, S. Yellampalli (Eds.) Carbon Nanotubes-Polymer Nanocomposites. InTech, 2011.

[5] D. Zhou, S. Seraphin, Complex branching phenomena in the growth of carbon nanotubes, Chem. Phys. Lett. 238 (1995) 286–289.

[6] D. Wei, Y. Liu, The intramolecular junctions of carbon nanotubes, Adv. Mater. 20 (2008) 2815–2841.

[7] G. Kwon K. Shin, B. Sung, Mixing molecular junctions with carbon nanotube-polymer composites: a strategy to enhance the conductivity and the transparency, J. Appl. Phys. Lett. 94 (2009) 193108.

[8] M. Terrones, A. G. Souza Filho, A. M. Rao, Doped carbon nanotubes: synthesis, characterization and applications. Carbon Nanotubes V: Topics in Applied Physics, Springer Berlin Heidelberg, 2008, pp. 531-566.

[9] A.V. Krasheninnikov, K. Nordlund, Irradiation effects in carbon nanotubes, NIM B: Beam Interactions with Mat. and Atoms 216 (2004) 355-366.

[10] B. Li, Y. Feng, K. Ding, G. Qian, X. Zhang, J. Zhang, The effect of gamma ray irradiation on the structure of graphite and multi-walled carbon nanotubes, Carbon 11 (2013) In Press, Accepted Manuscript .

[11] T. Filleter, H.D. Espinosa, Multi-scale mechanical improvement produced in carbon nanotube fibers by irradiation cross-linking, Carbon 56 (2013) 1-11.

[12] O. Lehtinen, L. Sun, T. Nikitin, A.V. Krasheninnikov, L. Khriachtchev, J.A. Rodríguez-Manzo, M. Terrones, F. Banhart, J. Keinonen. Ion irradiation of carbon nanotubes encapsulating cobalt crystal, Physica E: Low-dimensional Syst. and Nanostructures, 40 (2008) 2618-2621.

[13] A.G. Cano-Márquez, F.J. Rodríguez-Macías, J. Campos-Delgado, C.G. Espinosa-González, F. Tristán-López, D. Ramírez-González, D.A. Cullen, D.J. Smith, M. Terrones, Y.I. Vega-Cantú. Ex-MWNTs: graphene sheets and ribbons produced by lithium intercalation and exfoliation of carbon nanotubes. Nano Lett. 9 (2009) 1527-1533.

[14] K. Kardimi, T. Tsoufis, A. Tomou, B. J. Kooi, M. I. Prodromidis, D. Gournis, Synthesis and characterization of carbon nanotubes decorated with Pt and PtRu nanoparticles and assessment of their electrocatalytic performance, Int. J. Hydrogen Energy 37(2012) 1243-1253.

[15] Y. Liang, K. Wu, C. Ge, Y. Zhou, Y. Chen, Y. Tang, T. Lu, Efficient anchorage of palladium nanoparticles on the multi-walled carbon nanotubes as electrocatalyst for the hydrazine electrooxidation in strong acidic solutions, Fuel Cell 12 (2012) 946–955.

[16] J.W. Jang, C.E. Lee, S.C. Lyu, T.J. Lee, C.J. Lee, Structural study of nitrogen-doping effects in bamboo-shaped multiwalled carbon nanotubes, Appl. Phys. Lett. 84 (2004) 2877-2879.

[17] E.N. Nxumalo, N.J. Coville, Nitrogen doped carbon nanotubes from organometallic compounds: a review, Materials 3 (2010) 2141-2171.

[18] X. Ma, E. G. Wanga, CN_x/carbon nanotube junctions synthesized by microwave chemical vapor deposition. Appl. Phys. Lett. 78 (2001) 978-980.

[19] D. Wei, Y. Liu, L. Cao, L. Fu, X. Li, Y. Wang, G. Yu, D. Zhu, A new method to synthesize complicated multi-branched carbon nanotubes with controlled architecture and composition. Nano Lett. 6 (2006) 186-192.

[20] Q. Liu, W. Liu, Z.M. Cui, W.G. Song, L.J. Wan, Synthesis and characterization of 3D double-branched K junction carbon nanotubes and nanorods, Carbon 45 (2007) 268–273.

[21] B. Xiaodong, L. Dan, W. Ye, L. Ji, Effects of temperature and catalyst concentration on the growth of aligned carbon nanotubes, Tsingua Sci. Tech. 10 (2005) 729-735.

[22] C. Seah, S.P. Chai, A.R. Mohamed, Synthesis of aligned carbon nanotubes, Carbon 49 (2011) 4613–4635.

[23] Y. Lu, Z. Zhu, D. Su, D. Wang, Z. Liu, R. Schlo, Formation of bamboo-shape carbon nanotubes by controlled rapid decomposition of picric acid, Carbon 42 (2004) 3199–3207.

[24] A. Morelos-Gómez, F. López-Urías , E. Muñoz-Sandoval , C.L. Dennis , R.D. Shull , H. Terrones, M. Terrones. Controlling high coercivities of ferromagnetic nanowires encapsulated in carbon nanotubes. J. Mater. Chem. 20 (2010) 5906-5914.

[25] M.L. Garcia-Betancourt, S.M. Vega-Diaz, A. Morelos-Gomez, N. Perea-Lopez, R. Cruz-Silva, H. Gutierrez, H. Terrones, M. Terrones, and E. Muñoz-Sandoval, Synthesis of defective N-doped multiwall carbon nanotubs using water in the trap: morphology characterization, magnetic and electrical properties, accepted to Carbon 2013 conference.

[26] D. Meneses-Rodriguez, E. Munoz-Sandoval, G. Ramirez-Manzanares, D. Ramirez-Gonzalez, S. Diaz-Castanon, J. C. Faloh-Gandarilla, A. Morelos-Gomez, F. Lopez-Urias, M. Terrones, Magnetic Properties of Encapsulated Nanoparticles in Nitrogen-Doped Multiwalled Cabon Nanotubes Embedded in SiO_x Matrices. J. Nanosci. and Nanotech. 10 (2010) 5576-5582.

[27] F. Lopez-Urias, E. Munoz-Sandoval, M. Reyes-Reyes, A. H. Romero, M. Terrones, J. L. Moran-Lopez, Creation of Helical Vortices during Magnetization of Aligned Carbon Nanotubes. Phys. Rev. Lett. 94 (2005) 216102.

[28] H. M. Lu, W. T. Zheng,Q. Jiang, Saturation magnetization of ferromagnetic and ferromagnetic nanocrystals at room temperature. J. Phys. D-Appl. Phys. 40 (2007) 320-325.

[29] N. Grobert, W. K. Hsu, Y. Q. Zhu, J. P. Hare, H. W. Kroto, D. R. M. Walton, M. Terrones, H. Terrones, P. Redlich, M. Ruhle, R. Escudero, F. Morales, Enhanced magnetic coercivities in Fe nanowires. Appl. Phys. Lett. 75 (1999) 3363-3365.

[30] H. Terrones, F. Lopez-Urias, E. Munoz-Sandoval, J. A. Rodriguez-Manzo, A. Zamudio, A. L. Elias, M. Terrones, Magnetism in Fe-based and carbon nanostructures: Theory and applications. Solid State Sci. 8 (2006) 303-320.

[31] J. F. Marco, J. R. Gancedo, A. Hernando, P. Crespo, C. Prados, J. M. Gonzalez, N. Grobert, M. Terrones, D. R. M. Walton, H. W. Kroto, Mossbauer study of iron-containing carbon nanotubes. Hyperfine Interact. 139 (2002) 535-542.

[32] J. Jorge, E. Flahaut, F. Gonzalez-Jimenez, G. Gonzalez, J. Gonzalez, E. Belandria, J. M. Broto, B. Raquet, Preparation and characterization of alpha-Fe nanowires located inside double wall carbon nanotubes. Chem. Phys. Lett. 457 (2008) 347-351}

[33] H. Reuther, C. Mueller,A. Leonhardt, M. C. Kutz, Investigation of the Formation of Fe-filled Carbon Nanotubes. J. Phys. Conf. Ser. 217 (2010) 012098.

[34] S. V. Komogortsev, R. S. Iskhakov, A. D. Balaev, A. G. Kudashov, A. V. Okotrub, S. I. Smirnov, Magnetic properties of Fe_3C ferromagnetic nanoparticles encapsulated in carbon nanotubes. Phys. Solid State 49 (2007) 734-738